Revision 1

Supplementary materials

Effect of cationic substitution on the pressure-induced Calcium carbonate phase transitions

Martirosyan N.S.[1,2], Efthimiopoulos I.[1], Pennacchioni L.[1,3], Wirth R. [1], Jahn S.[2], Koch-Müller M.[1]

[1] GFZ German Research Centre for Geosciences, Telegrafenberg, 14473 Potsdam, Germany

[2] Institute of Geology and Mineralogy, University of Cologne, Zülpicher Str. 49b, 50674 Cologne, Germany

[3] Institute of Geosciences, Goethe University, Altenhöferallee 1, D-60438 Frankfurt am Main, Germany

*Corresponding author: martirosyanns@gmail.com

Content

and fourth experimental runs measurements were performed only on compression (1-st P increase). Colors and black text represent phases detected at each P point (also shown in the legend). The six high P phases of (Ca, Sr)CO_3 were detected at room T: Sr-calcite-II (Sr-CC-II); Sr-calcite-IIIb (Sr-CC-IIIb); Sr-calcite-III (Sr-CC-III); Sr-calcite-IIIc (Sr-CC- IIIc); Sr-calcite-VII (Sr-CC-VII); Sr-post-aragonite (Sr-Post-Arag). Gray lines and text show phase transitions in pure $CaCO_3$ at room temperature from previous studies (Pippinger et al., 2014; Koch-Müller et al., 2016; Bayarjargal et al., 2018).

Fig. S2. BSE images of the synthesized $Ca_{0.82}Sr_{0.18}CO_3$ solid solution. (a) overview of the synthesized grains (b) closer look, showing the homogeneous main $Ca_{0.82}Sr_{0.18}CO_3$ carbonate (gray) and small inclusions of secondary phase (marked by arrows).

Fig. S3. TEM High – angel annular dark – field (HAADF) image of the sample (a) and the EDX spectra: (b) – inclusion of the Sr-rich carbonate; (c) – main phase.

Fig. S4. Refined MID infrared spectrum of the $Ca_{0.82}Sr_{0.18}CO_3$ solid solution (Sr-calcite-II) in the range of 600 – 1100 cm^{-1} wavenumbers. The ν_3 band located at 1200 cm^{-1} is oversaturated and cannot be unequivocally fitted.

Fig. S5. Raman spectrum of $Ca_{0.82}Sr_{0.18}CO_3$ solid solution at atmospheric P (Sr-calcite-II) in comparison with reference spectra of pure $CaCO_3$ calcite (RUFF R050127) and Ca-strontianite $Sr_{0.91}Ca_{0.09}CO_3$ (RUFF R040037). Fundamental Raman modes are marked on the figure: symmetric stretching (ν_1), out-of-plane bending (ν_2), in-plane bending (ν_4) and lattice vibrations (LV) (White, 1974). Arrows show the additional modes arising in the Sr-calcite-II. For more details see Fig. S6

Fig. S6. Refined Raman spectrum of $Ca_{0.82}Sr_{0.18}CO_3$ solid solution at atmospheric pressure (Sr-calcite-II) in the range of 200 – 900 cm^{-1} wavenumbers. The experimental spectrum is represented by green line; refined positions of the bands – red line. The main bands are additionally marked with numbers.

Fig. S7. Evolution of the Raman mode frequencies with pressure at 0 – 18 GPa in the range of 1080 – 1170 cm^{-1}. The vertical dashed lines represent the onset of various transitions. Bands of the different phases are marked with colors and symbols: Sr-calcite-II (Sr-CC-II) – white square; Sr-CC-IIIb (Sr-CC-IIIb) – green triangles; Sr-CC-III and IIIc (Sr-CC-III, IIIc) –

blue and purple diamonds, respectively; Sr-calcite-VII (Sr-CC-VII) – black circles. All point were obtained from the Raman spectra measured in the run 3 (for more details see Fig.S1).

Fig. S8. Representative spectra of Sr-calcite-III (a), IIIc (b) and IIIb (c) in the range of 1060-1140 cm^{-1}. Spectrum (a) was collected upon compression (run 3, Fig. S1). Spectra (b) and (c) were collected upon decompression at 7 GPa (run 1 in Fig. S1). The red curves represent the refined modes.

Fig. S9. Representative spectra of Sr-calcite-IIIb (a), III (b) and IIIc (c) in the range of 200-900 cm^{-1}. All spectra were collected upon compression (run 3 in Fig. S1). The red curves represent the refined modes.

Fig. S10. Evolution of the Raman mode frequencies with pressure above 20 GPa in the range of 700 – 1220 cm^{-1}. Band of the Sr-calcite-VII (Sr-CC-VII) are marked with black circles. The bands of Sr-post-aragonite are presented with red circles. All point were obtained from the Raman spectra measured in the run 3 (for more details see Fig.S1).

Fig. S11. Refined Raman spectrum of Sr-calcite-VII (Sr-CC-VII) at 34.6 GPa (run 3, Fig. S1) in the range of 200 – 900 cm^{-1}. The experimental spectrum is represented by green line; refined positions of the bands – red line. The main bands are additionally marked with numbers.

Fig. S12. Comparison of Raman spectrum of Sr-calcite-VII collected in this study at 34.6 GPa (red) and the Raman spectra of $CaCO_3$-VI and VII from (Bayarjargal et al., 2018). Raman spectrum of $CaCO_3$-VI contains a single ν_2 band (870 cm^{-1} at 30 GPa), while in $CaCO_3$-VII and Sr-calcite-VII two distinct bands at 850 – 890 cm^{-1} could be observed.

Fig. S13. Raman spectra collected in the high T experiments: (a, b) before and during the heating and (c, d) after quenching to atmospheric pressure. Spectra presented on (c, d) were collected from different parts of the sample. Abbreviations: Sr-CC-II – Sr-calcite-II; Sr-CC-IIIb, and IIIc – Sr-calcite-IIIb, and IIIc, respectively; Sr-Arag – Sr-aragonite.

Experimental methods.

Temperature calibration in DAC

Pressure (P) and temperature (T) inside the sample chamber in the high T diamond anvil cell (DAC-HT) experiments were measured using $SrB_4O_7:Sm^{2+}$ and ruby. Due to the negligible effect of T on the $^7D_0 \rightarrow {}^5F_0$ fluorescence line of the $SrB_4O_7:Sm^{2+}$ below 770 K and 35 GPa (Rashchenko et al., 2015), a chip of $SrB_4O_7:Sm^{2+}$ was used to define the P. On the contrary, the position of R1 ruby fluorescence peak depends both on P and T. Once the P was determined with the $SrB_4O_7:Sm^{2+}$, the shift of the ruby R1 line at room T was computed, showing the contribution of P to the measured total shift. The contribution of T was then estimated by subtracting calculated position of the R1 peak at room T from the measured total shift (Datchi et al., 2007).

Table S1. Composition of the recovered phase measured by microprobe analyses. Average compositions and standard deviations (in brackets) are given based on 18 measurements.

	Phase	CaO	SrO	MgO	Total
			wt%		
Sample	Sr-Cal	42.15 (1.20)	17.42 (1.46)	-	59.57

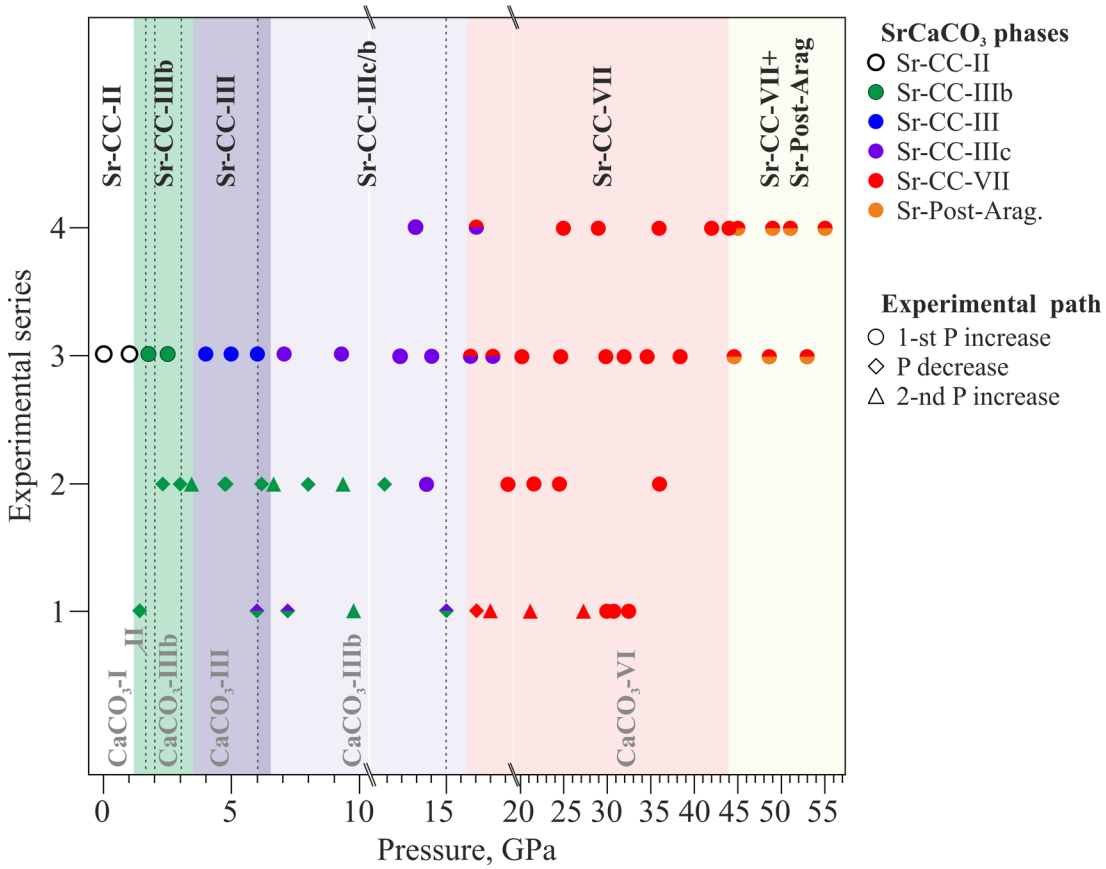

Fig. S1. Experimental conditions and results of the in situ high P Raman study at room T. We carried out four different high P experimental series, each indicated on the left axes. Measurements were conducted on different P path. In the first experimental run P was increased from 30.0 to 32.5 GPa (1-st P increase), then decreased gradually to 1.5 GPa (P decrease) and increased again (2-nd P increase). The same procedure was used for the second run. In the third and fourth experimental runs measurements were performed only on compression (1-st P increase). Colors and black text represent phases detected at each P point (also shown in the legend). The six high P phases of (Ca, Sr)CO_3 were detected at room T: Sr-calcite-II (Sr-CC-II); Sr-calcite-IIIb (Sr-CC-IIIb); Sr-calcite-III (Sr-CC-III); Sr-calcite-IIIc (Sr-CC- IIIc); Sr-calcite-VII (Sr-CC-VII); Sr-post-aragonite (Sr-Post-Arag). Gray lines and text show phase transitions in pure $CaCO_3$ at room temperature from previous studies (Pippinger et al., 2014; Koch-Müller et al., 2016; Bayarjargal et al., 2018).

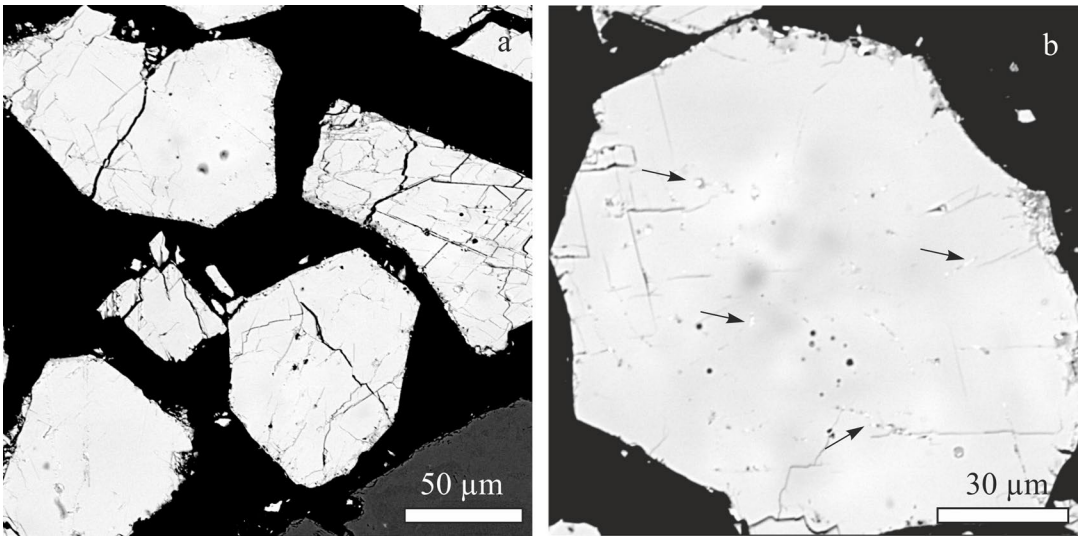

Fig. S2. BSE images of the synthesized $Ca_{0.82}Sr_{0.18}CO_3$ solid solution. (a) overview of the synthesized grains (b) closer look, showing the homogeneous main $Ca_{0.82}Sr_{0.18}CO_3$ carbonate (gray) and small inclusions of secondary phase (marked by arrows).

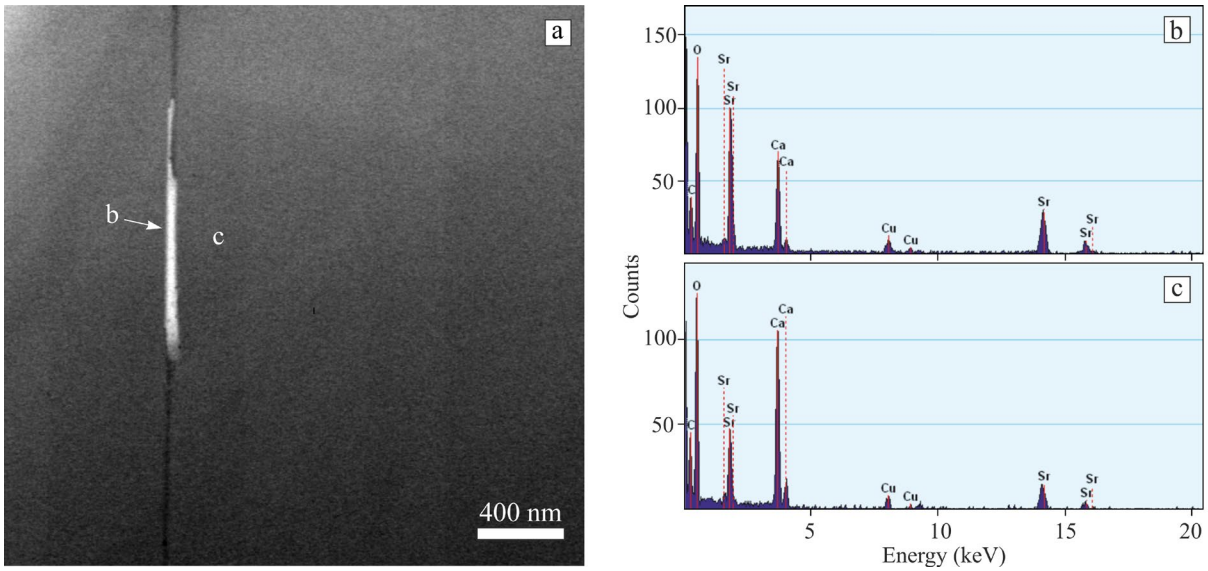

Fig. S3. TEM High – angel annular dark – field (HAADF) image of the sample (a) and the EDX spectra: (b) – inclusion of the Sr-rich carbonate; (c) – main phase.

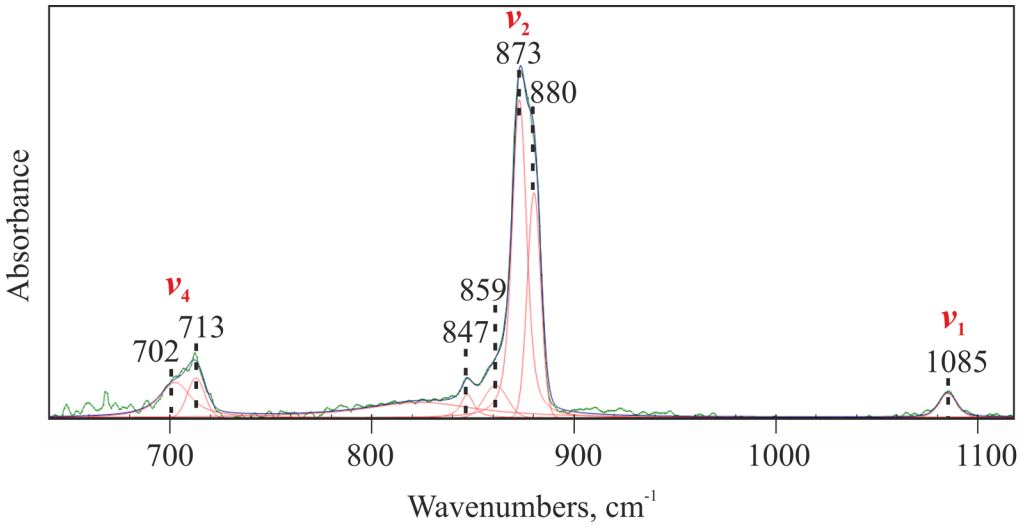

Fig. S4. Refined MID infrared spectrum of the $Ca_{0.82}Sr_{0.18}CO_3$ solid solution (Sr-calcite-II) in the range of 600 – 1100 cm^{-1} wavenumbers. The ν_3 band located at 1200 cm^{-1} is oversaturated and cannot be unequivocally fitted.

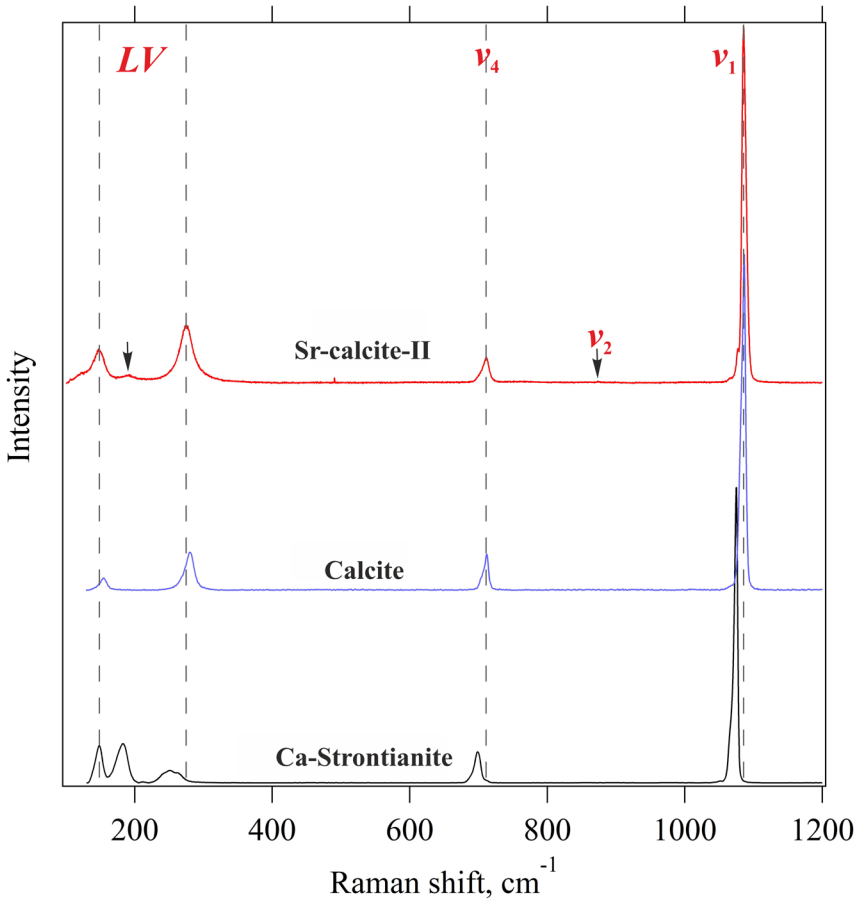

Fig. S5. Raman spectrum of $Ca_{0.82}Sr_{0.18}CO_3$ solid solution at atmospheric P (Sr-calcite-II) in comparison with reference spectra of pure $CaCO_3$ calcite (RUFF R050127) and Ca-strontianite $Sr_{0.91}Ca_{0.09}CO_3$ (RUFF R040037). Fundamental Raman modes are marked on the figure: symmetric stretching (ν_1), out-of-plane bending (ν_2), in-plane bending (ν_4) and lattice vibrations (LV) (White, 1974). Arrows show the additional modes arising in the Sr-calcite-II. For more details see Fig. S6

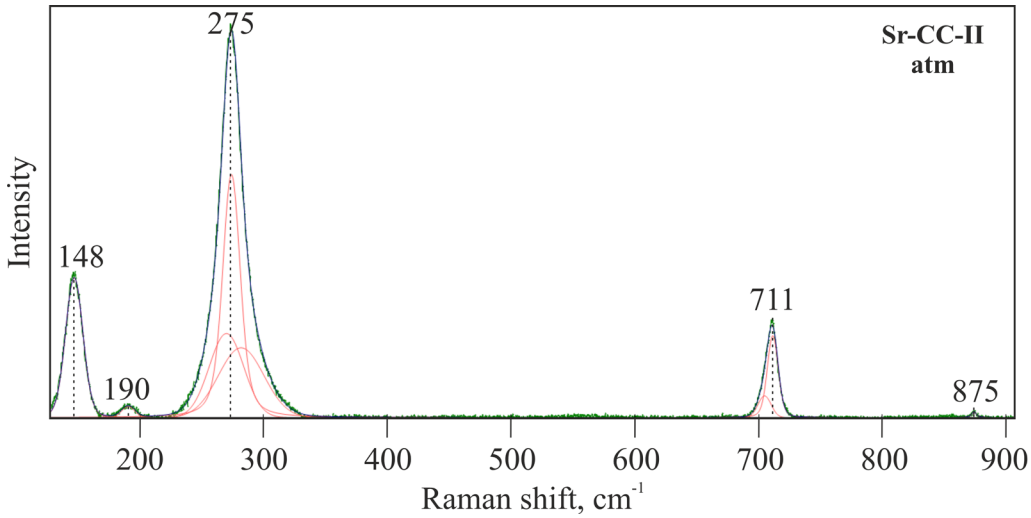

Fig. S6. Refined Raman spectrum of $Ca_{0.82}Sr_{0.18}CO_3$ solid solution at atmospheric pressure (Sr-calcite-II) in the range of 200 – 900 cm^{-1} wavenumbers. The experimental spectrum is represented by green line; refined positions of the bands – red line. The main bands are additionally marked with numbers.

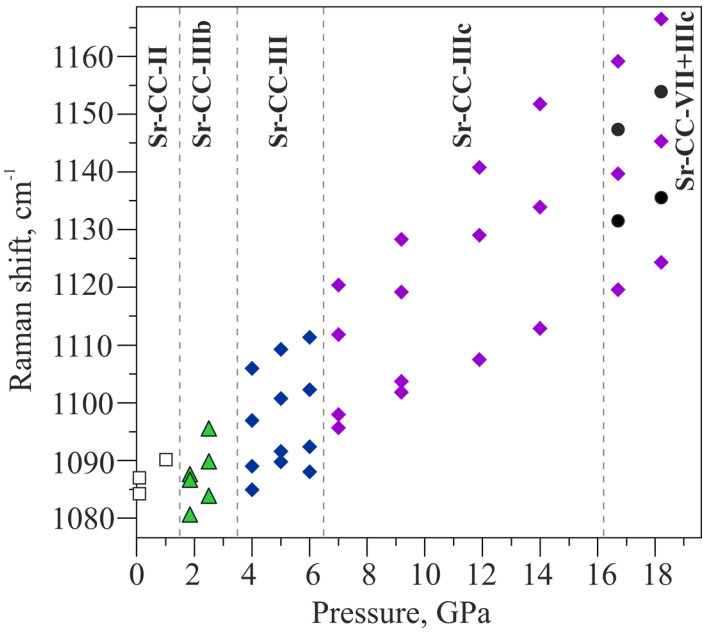

Fig. S7. Evolution of the Raman mode frequencies with pressure at 0 – 18 GPa in the range of 1080 – 1170 cm^{-1}. The vertical dashed lines represent the onset of various transitions. Bands of the different phases are marked with colors and symbols: Sr-calcite-II (Sr-CC-II) – white square; Sr-CC-IIIb (Sr-CC-IIIb) – green triangles; Sr-CC-III and IIIc (Sr-CC-III, IIIc) – blue and purple diamonds, respectively; Sr-calcite-VII (Sr-CC-VII) – black circles. All point were obtained from the Raman spectra measured in the run 3 (for more details see Fig.S1).

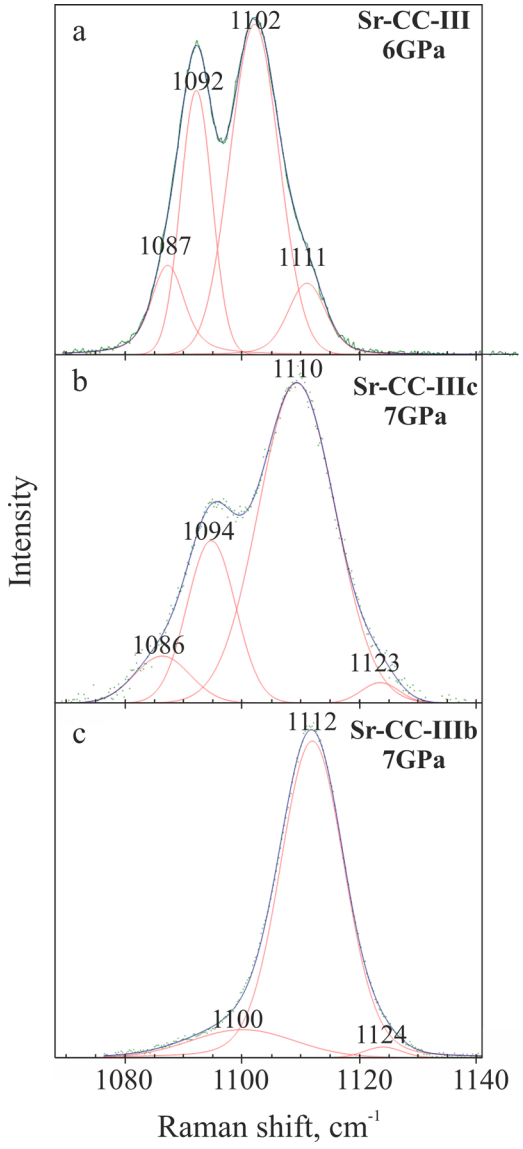

Fig. S8. Representative spectra of Sr-calcite-III (a), IIIc (b) and IIIb (c) in the range of 1060-1140 cm^{-1}. Spectrum (a) was collected upon compression (run 3, Fig. S1). Spectra (b) and (c) were collected upon decompression at 7 GPa (run 1 in Fig. S1). The red curves represent the refined modes.

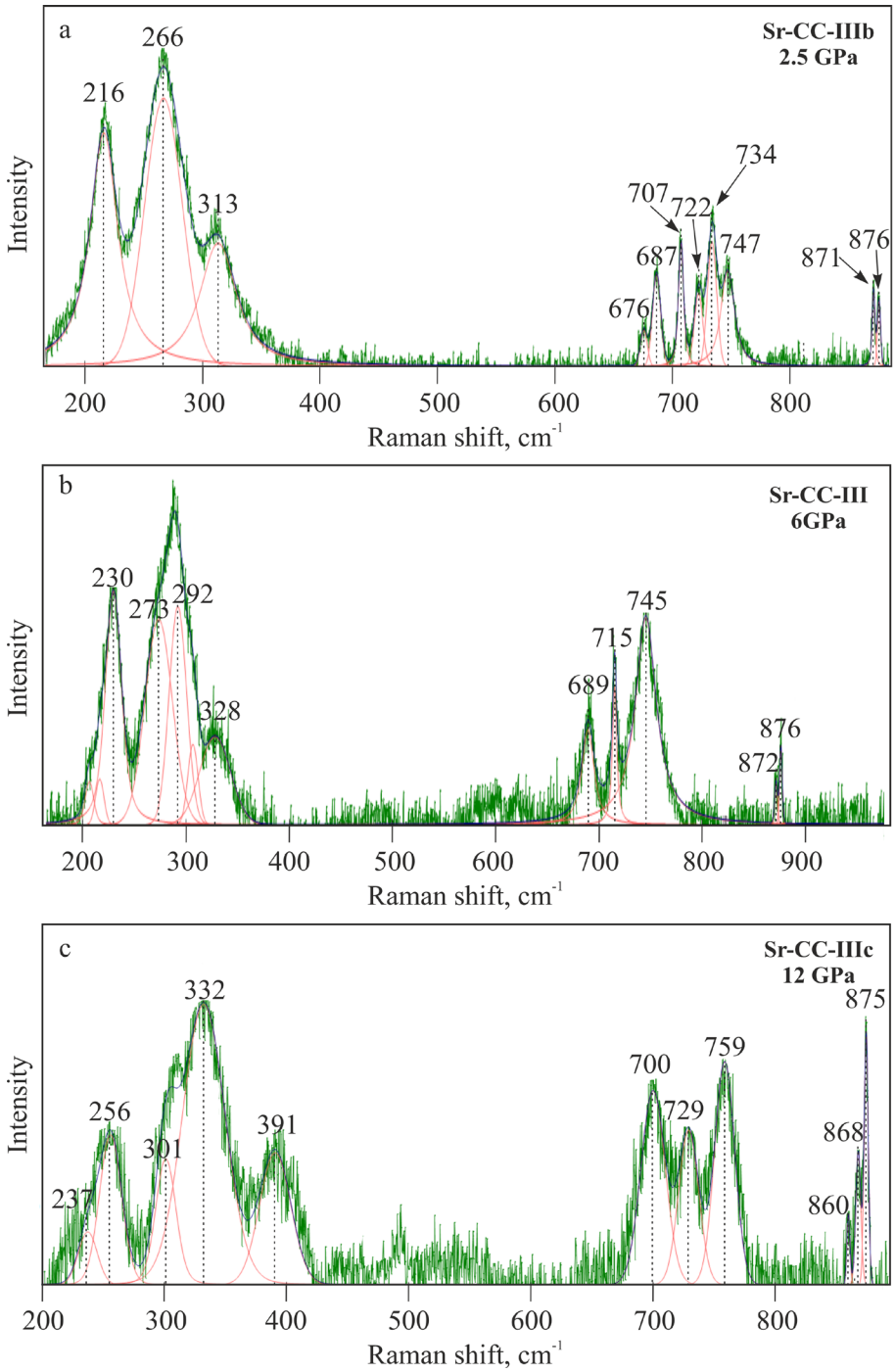

Fig. S9. Representative spectra of Sr-calcite-IIIb (a), III (b) and IIIc (c) in the range of 200-900 cm^{-1}. All spectra were collected upon compression (run 3 in Fig. S1). The red curves represent the refined modes.

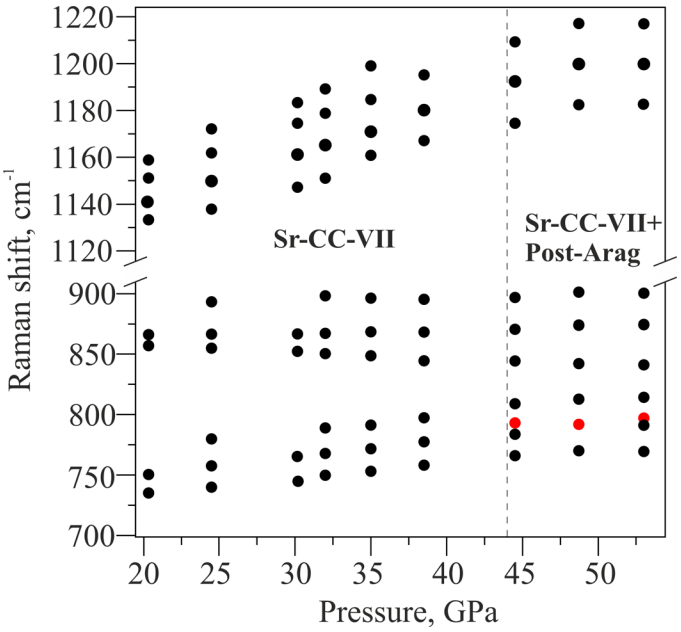

Fig. S10. Evolution of the Raman mode frequencies with pressure above 20 GPa in the range of 700 – 1220 cm^{-1}. Band of the Sr-calcite-VII (Sr-CC-VII) are marked with black circles. The bands of Sr-post-aragonite are presented with red circles. All point were obtained from the Raman spectra measured in the run 3 (for more details see Fig.S1).

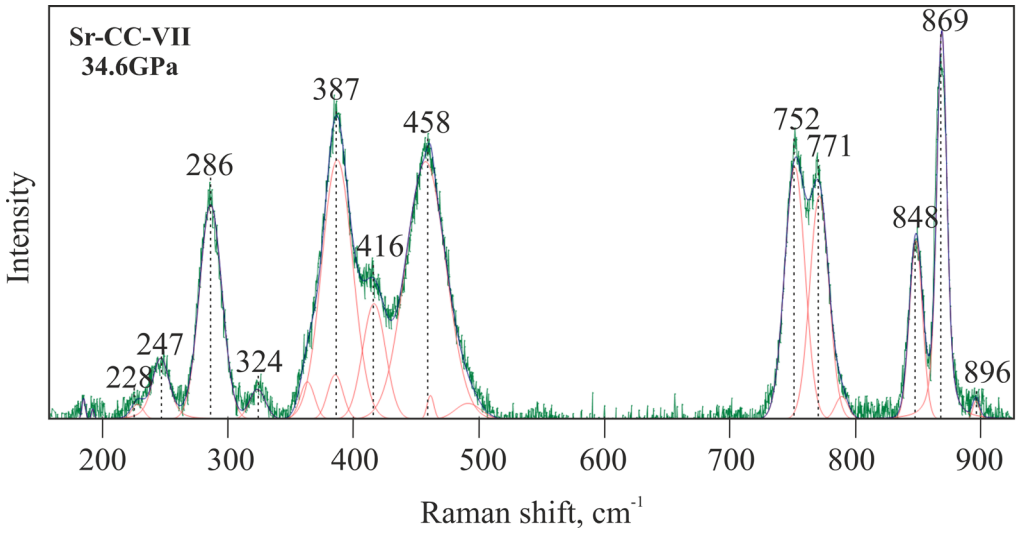

Fig. S11. Refined Raman spectrum of Sr-calcite-VII (Sr-CC-VII) at 34.6 GPa (run 3, Fig. S1) in the range of 200 – 900 cm^{-1}. The experimental spectrum is represented by green line; refined positions of the bands – red line. The main bands are additionally marked with numbers.

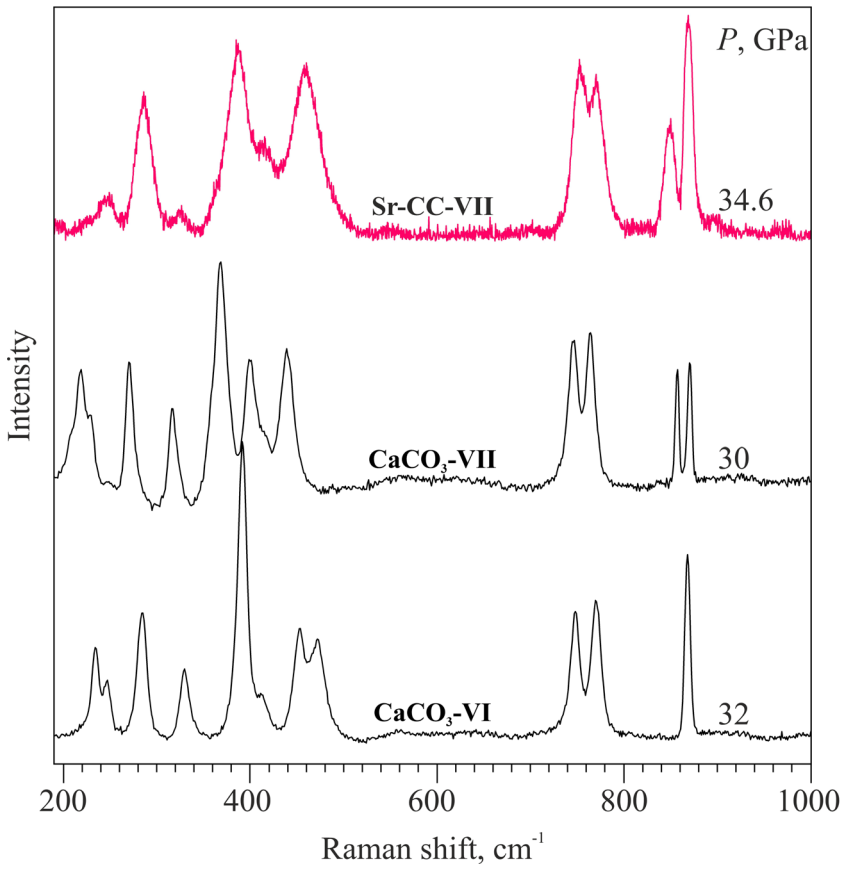

Fig. S12. Comparison of Raman spectrum of Sr-calcite-VII collected in this study at 34.6 GPa (red) and the Raman spectra of $CaCO_3$-VI and VII from (Bayarjargal et al., 2018). Raman spectrum of $CaCO_3$-VI contains a single ν_2 band (870 cm^{-1} at 30 GPa), while in $CaCO_3$-VII and Sr-calcite-VII two distinct bands at 850 – 890 cm^{-1} could be observed.

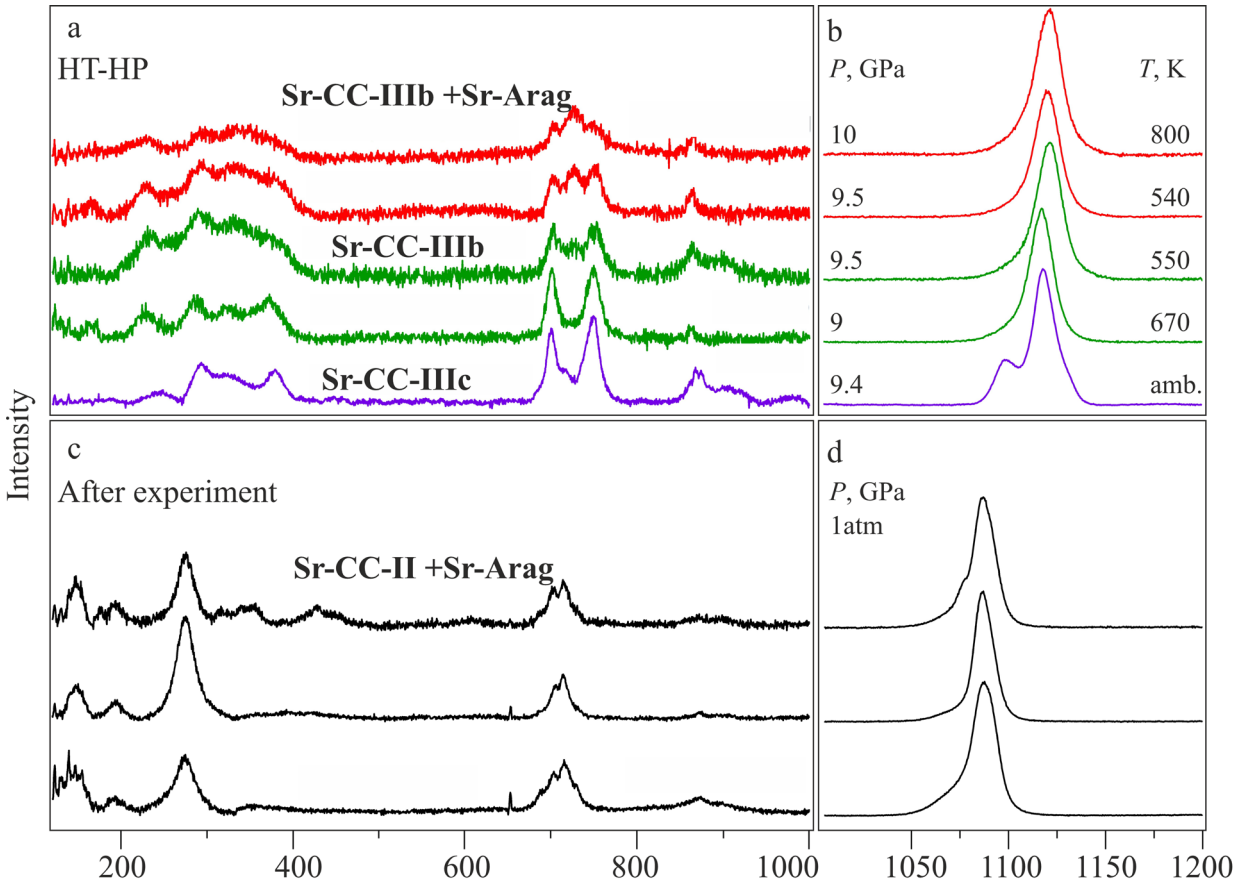

Fig. S13. Raman spectra collected in the high T experiments: (a, b) before and during the heating and (c, d) after quenching to atmospheric pressure. Spectra presented on (c, d) were collected from different parts of the sample. Abbreviations: Sr-CC-II – Sr-calcite-II; Sr-CC-IIIb, and IIIc – Sr-calcite-IIIb, and IIIc, respectively; Sr-Arag – Sr-aragonite.

References

Bayarjargal, L., Fruhner, C.J., Schrodt, N., Winkler, B., 2018. CaCO3 phase diagram studied with Raman spectroscopy at pressures up to 50 GPa and high temperatures and DFT modeling. Physics of the Earth and Planetary Interiors, 281: 31-45.

Datchi, F., Dewaele, A., Loubeyre, P., Letoullec, R., Le Godec, Y., Canny, B., 2007. Optical pressure sensors for high-pressure–high-temperature studies in a diamond anvil cell. High Pressure Research, 27: 447-463.

Koch-Müller, M., Jahn, S., Birkholz, N., Ritter, E., Schade, U., 2016. Phase transitions in the system CaCO3 at high P and T determined by in situ vibrational spectroscopy in diamond anvil cells and first-principles simulations. Physics and Chemistry of Minerals, 43: 545-561.

Pippinger, T., Miletich, R., Merlini, M., Lotti, P., Schouwink, P., Yagi, T., Crichton, W.A., Hanfland, M., 2014. Puzzling calcite-III dimorphism: crystallography, high-pressure behavior, and pathway of single-crystal transitions. Physics and Chemistry of Minerals, 42: 29-43.

Rashchenko, S.V., Kurnosov, A., Dubrovinsky, L., Litasov, K.D., 2015. Revised calibration of the Sm: SrB4O7 pressure sensor using the Sm-doped yttrium-aluminum garnet primary pressure scale. Journal of Applied Physics, 117: 145902.

White, W., 1974. The carbonate minerals: In The Infrared Spectra of Minerals (Edited by VC Farmer). Mineralogical Society, London.

Wirth, R., 2009. Focused Ion Beam (FIB) combined with SEM and TEM: Advanced analytical tools for studies of chemical composition, microstructure and crystal structure in geomaterials on a nanometre scale. Chemical Geology, 261: 217-229.

Wojdyr, M., 2010. Fityk: a general-purpose peak fitting program. Journal of Applied Crystallography, 43: 1126-1128.